



Lawrence Berkeley Laboratory

UNIVERSITY OF CALIFORNIA

Materials & Molecular Research Division

Submitted to the Journal of Chemical Physics

OPTICAL SPECTRA AND ZEEMAN EFFECT FOR Er^{3+} IN
 LuPO_4 AND HfSiO_4

T. Hayhurst, G. Shalimoff, N. Edelstein,
L.A. Boatner, and M.M. Abraham

January 1981

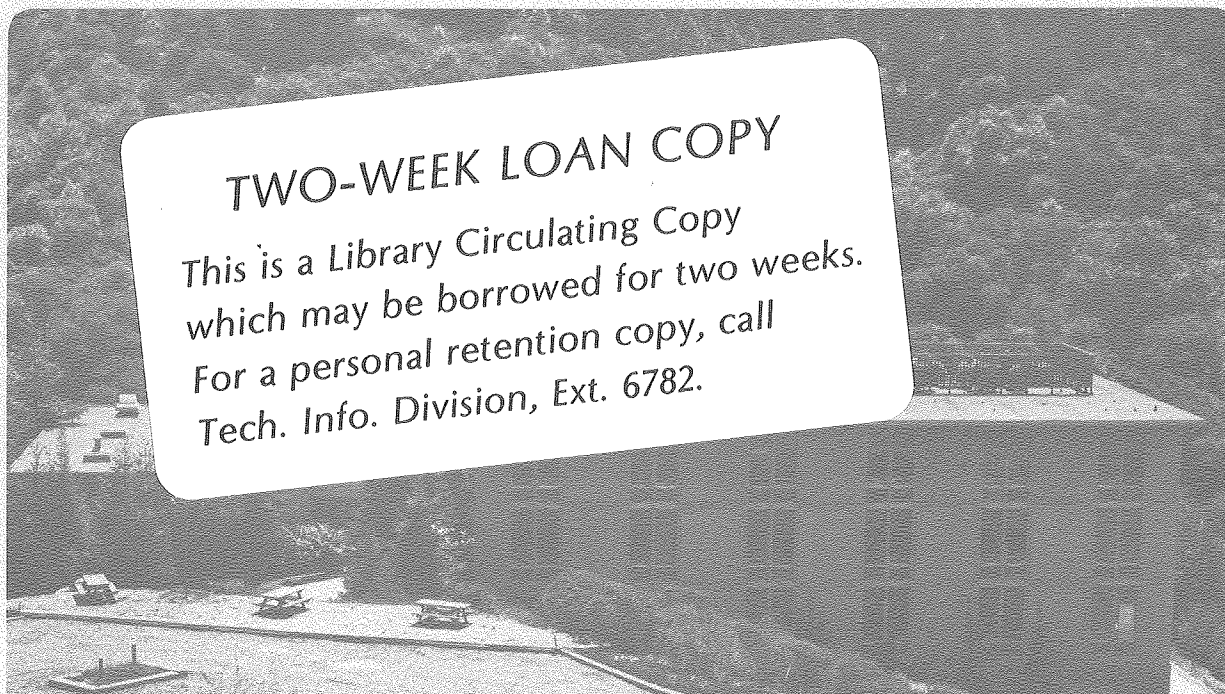
RECEIVED
LAWRENCE
BERKELEY LABORATORY

MAR 24 1981

LIBRARY AND
DOCUMENTS SECTION

TWO-WEEK LOAN COPY

This is a Library Circulating Copy
which may be borrowed for two weeks.
For a personal retention copy, call
Tech. Info. Division, Ext. 6782.



LBL-11943 and

DISCLAIMER

This document was prepared as an account of work sponsored by the United States Government. While this document is believed to contain correct information, neither the United States Government nor any agency thereof, nor the Regents of the University of California, nor any of their employees, makes any warranty, express or implied, or assumes any legal responsibility for the accuracy, completeness, or usefulness of any information, apparatus, product, or process disclosed, or represents that its use would not infringe privately owned rights. Reference herein to any specific commercial product, process, or service by its trade name, trademark, manufacturer, or otherwise, does not necessarily constitute or imply its endorsement, recommendation, or favoring by the United States Government or any agency thereof, or the Regents of the University of California. The views and opinions of authors expressed herein do not necessarily state or reflect those of the United States Government or any agency thereof or the Regents of the University of California.

OPTICAL SPECTRA AND ZEEMAN EFFECT FOR Er^{3+} IN LuPO_4 AND HfSiO_4

T. Hayhurst, G. Shalimoff, and N. Edelstein
Materials and Molecular Research Division
Lawrence Berkeley Laboratory
University of California, Berkeley 94720

and

L. A. Boatner and M. M. Abraham
Solid State Division, Oak Ridge National Laboratory
Oak Ridge, Tennessee 37830

ABSTRACT

The absorption spectra of Er^{3+} diluted in LuPO_4 and HfSiO_4 crystals have been measured from 6,000 to 28000 cm^{-1} at liquid He and N_2 temperatures. Zeeman spectra were obtained in the visible region. The transitions were assigned and fitted to a semiempirical Hamiltonian with ten adjustable parameters. Satisfactory fits were obtained including reasonable agreement between calculated and measured g values.

INTRODUCTION

The relatively long half-lives (10^3 to 10^5 yr) of many of the actinide isotopes produced as a by-product of nuclear reactor operation represent a severe constraint on the selection of a suitable substance for the primary isolation or containment of nuclear wastes. An examination of geological evidence has recently led to the suggestion^{1,2} that synthetic analogs of the mineral monazite $[(\text{La}, \text{Ce}, \text{Nd}, \text{Y}, \dots)\text{PO}_4]$ have chemical and physical properties that make them attractive candidates as host materials for long-term storage of actinide wastes. Accordingly, the characterization of possible sites where actinide (and other) impurity ions can be incorporated in these materials and a determination of the oxidation states of these ions is pertinent to understanding the interrelationship between the chemical and physical properties of the lanthanide orthophosphate-impurity systems and the parameters appropriate to an acceptable stable waste form.

The pure lanthanide orthophosphates are structurally divided into two classes: the first half of the series (LaPO_4 to GdPO_4) has the monoclinic monazite structure, while the second half of the series (TbPO_4 to LuPO_4 , plus YPO_4 , and ScPO_4) is characterized by the tetragonal zircon structure. Previous work using the electron paramagnetic resonance (EPR) technique with the lanthanide ion Gd^{3+} employed as a probe has shown that this ion occupies identical substitutional sites in both single crystal and powder samples in either the tetragonal or monoclinic symmetry orthophosphates.³⁻⁵ More recent EPR investigations^{6,7} have been carried out for other lanthanides that are either direct analogs of or have properties that are directly

related to the actinide ions of interest. These studies have included work on Ce^{3+} , Nd^{3+} , Dy^{3+} , Er^{3+} , and Yb^{3+} in the tetragonal-symmetry hosts LuPO_4 , YPO_4 , and ScPO_4 . In the present work the results of complementary optical absorption and Zeeman effect studies are reported in the range from 0.4 to 3.0 nm for Er^{3+} as a dilute impurity in LuPO_4 . Energy levels were assigned to states derived from the constraint of an f^{11} configuration restricted to D_{2d} point symmetry, and were fit to a semiempirical Hamiltonian by a least-squares minimization. Parameters describing the electrostatic, spin-orbit, and crystal field interactions were adjusted. Results of this analysis, along with the previously reported EPR measurements, were used to assign the optical spectra of Er^{3+} in HfSiO_4 that are also reported here. Although hafnium silicate is isostructural with LuPO_4 , it appears that the trivalent Er ion can substitute into more than one site in the silicate host crystal.⁸ By a close comparison with the $\text{Er}^{3+}:\text{LuPO}_4$ system, the spectra associated with only the D_{2d} site were assigned and good agreement was obtained between the experimental and calculated energy levels. The crystal field parameters reported here provide a basis for future work on tetrapositive actinide ions (e.g., Np^{4+}) in this type of host crystal.

EXPERIMENTAL PROCEDURE

The preparation⁹ and EPR characterization⁸ of the Er-doped HfSiO_4 crystals have been reported elsewhere. The Er-doped LuPO_4 single crystals employed in this work were grown by a technique^{4,5}

similar to that initially described by Feigelson.¹⁰ In this procedure the lanthanide oxide (i.e., Lu_2O_3 plus the Er_2O_3 dopant) is mixed with PbHPO_4 and reacted at high temperature (1360°C) in a platinum crucible. Accompanying decomposition of the PbHPO_4 results in the formation of $\text{Pb}_2\text{P}_2\text{O}_7$, which then serves as a flux during the subsequent crystal growth via spontaneous nucleation during slow cooling (1°C/h).

The absorption spectra were observed by detecting the transmitted light from a 100 watt tungsten-halogen lamp. Transitions between 12,000 and 28,000 cm^{-1} were photographed on a 3.4m Ebert spectrograph with a dispersion of about 5.2 $\text{\AA}/\text{mm}$, while the transitions between 6,000 and 12,000 cm^{-1} were observed using a 0.5 m Jarrel-Ash scanning monochromator equipped with a PbS detector. The observations were made at 4.2°K and 77°K in the visible region and at 2.0°K and 77°K in the infrared region. In each case the light was analyzed with a linear polarizer oriented in both the parallel and perpendicular directions relative to the c axis of the crystal. The photographic measurements were then repeated at 4.2°K with the crystal in a magnetic field of about 26 kG, with the c axis parallel and perpendicular to the applied magnetic field.

ANALYSIS AND DISCUSSION

The electronic states resulting from an f^n configuration restricted to D_{2d} symmetry can be described by means of an effective Hamiltonian of the following form:¹¹

4,

$$H = H_1 + H_2 + H_3 + H_4$$

where

$$H_1 = \sum_{k=0,2,4,6} p^k \left(\sum_{j>i=1}^n \sum_{q=-k}^k (-1)^q c_q^k(i) c_{-q}^k(j) \right)$$

$$H_2 = \zeta \sum_{i=1}^n \vec{L}_i \cdot \vec{S}_i$$

$$H_3 = \sum_{i=1}^n (B_0^2 C_0^2(i) + B_0^4 C_0^4(i) + B_4^4 [C_4^4(i) + C_{-4}^4(i)] \\ + B_4^6 [C_4^6(i) + C_{-4}^6(i)])$$

and H_4 contains configuration interaction terms including α , β , γ , three body interactions (T_k), and additional magnetic terms (M_k , P_k).¹²

The crystal field states for an odd number of electrons are classified by the Γ_6 and Γ_7 double group representations associated with the D_{2d} site symmetry. The selection rules for electric dipole representations among the Γ_6 , Γ_7 states for linear polarized incident light are given by:

$$\Gamma_6(\Gamma_7) \rightarrow \Gamma_7(\Gamma_6) \quad (\text{pol.} \parallel C)$$

$$\Gamma_6(\Gamma_7) \rightarrow \Gamma_6, \Gamma_7 \quad (\text{pol.} \perp C)$$

These selection rules are clearly obeyed by the $\text{Er}^{3+}:\text{LuPO}_4$ system as they are in previously reported $\text{Er}^{3+}:\text{YPO}_4$ spectra.¹³ This was not the case, however, for the $\text{Er}^{3+}:\text{HfSiO}_4$ crystals that were used in this study. Extra lines in the absorption spectrum of HfSiO_4 are observed due to

additional sites occupied by the Er^{3+} ion. In addition, the transmission of polarized light through the HfSiO_4 crystals indicated that the particular crystals used must be partially polycrystalline.

Because of the nearly identical structures of LuPO_4 and YPO_4 , the spectra of $\text{Er}^{3+}:\text{LuPO}_4$ were first assigned by correspondence with those of $\text{Er}^{3+}:\text{YPO}_4$.¹³ The semi-empirical Hamiltonian was then fitted to each system by least squares minimization of the parameters associated with H_1 , H_2 , and H_3 . The fit to $\text{Er}^{3+}:\text{YPO}_4$ served to test the model and the assignments of $\text{Er}^{3+}:\text{LuPO}_4$. The assignments were then refined and confirmed by comparing the calculated and measured g values where magnetic field splittings could be observed. This procedure was then applied to the $\text{Er}^{3+}:\text{HfSiO}_4$ spectra by careful comparison with both the $\text{Er}^{3+}:\text{LuPO}_4$ and $\text{Er}^{3+}:\text{YPO}_4$ assignments.

Satisfactory fits were obtained in all three cases. Fifty-five transitions were assigned to crystal field levels from the $\text{Er}^{3+}:\text{LuPO}_4$ spectra while 46 transitions were assigned from the $\text{Er}^{3+}:\text{HfSiO}_4$ spectra. The free ion parameters associated with H_4 were relatively insensitive to these data and could not be adjusted by the least squares procedure. Better agreement was obtained, however, when these parameters were left at their $\text{Er}^{3+}:\text{LaCl}_3$ values than when removed from the Hamiltonian.

The observed and calculated values of the energies and g-values for Er^{3+} in LuPO_4 and HfSiO_4 appear in Table I, while the values of the parameters determined for all three crystals appear in Table II. The agreement between the calculated g values and the g values observed from EPR measurements^{6,7,14,15} for the ground state of $\text{Er}^{3+}:\text{HfSiO}_4$ is especially gratifying, as these values are quite different from those observed for

Er^{3+} in LuPO_4 and Er^{3+} in YPO_4 .

The $4f^{11}$ electronic configuration of Er^{3+} can be viewed as representing three holes in the $4f^{14}$ closed shell and, accordingly the spectroscopic properties of this ion are of interest for comparison with those of Nd^{3+} , U^{3+} , and Np^{4+} which have three electrons in f shells. For the purpose of making comparisons of this type, studies of Nd^{3+} and U^{3+} in the lanthanide orthophosphates are currently in progress.

Acknowledgments

This work was supported at LBL by the Division of Chemical Sciences, Office of Basic Energy Sciences, U.S. Department of Energy under Contract No. W-7405-Eng-48. Oak Ridge National Laboratory is operated by Union Carbide Corporation for the U.S. Department of Energy under Contract W-7405-Eng-26.

References

1. L.A. Boatner, G.W. Beall, M.M. Abraham, C.B. Finch, P.G. Huray, and M. Rappaz, in The Scientific Basis for Nuclear Waste Management, Vol. II, p. 298, C.J. Northrup, Ed., (Plenum Press), 1980.
2. L.A. Boatner, G.W. Beall, M.M. Abraham, C.B. Finch, R.J. Floran, P.G. Huray and M. Rappaz, in The Management of Alpha-Contaminated Wastes, IAEA-SM-246/73, International Atomic Energy Agency, Vienna, Austria (in press).
3. M.M. Abraham, L.A. Boatner, T.C. Quinby, D.K. Thomas and M. Rappaz, Radioactive Waste Management, Vol. I, No. 2 (in press).
4. M. Rappaz, L.A. Boatner and M.M. Abraham, J. Chem. Phys. 73, 1095 (1980).
5. M. Rappaz, M. Abraham, J.O. Ramey, and L.A. Boatner, Phys. Rev. B 23, 0000 (1981).
6. L.A. Boatner, M. Rappaz and M.M. Abraham, in The Scientific Basis for Nuclear Waste Management, vol. III, J.G. Moore, Ed., (Plenum Press), 1981.
7. M.M. Abraham, L.A. Boatner, and M. Rappaz, in Nuclear and Electron Resonance Spectroscopies Applied to Materials Science, E.N. Kaufmann and G.K. Shenoy, Eds., (Elsevier North Holland), 1981.
8. R.W. Reynolds, L.A. Boatner, C.B. Finch, A. Chatelain, and M.M. Abraham, J. Chem. Phys. 56, 5607 (1972).
9. C.B. Finch, L.A. Harris and G.W. Clark, Am. Mineralogist 49, 782 (1964).
10. R.S. Feigelson, J. Am. Ceram. Soc. 47, 257 (1964).

11. B.G. Wybourne, Spectroscopic Properties of the Rare Earths, John Wiley & Sons (1965).
12. W.T. Carnall, H.C. Crosswhite, and H.M. Crosswhite, "Energy Level Structure and Transition Probabilities in the Spectra of the Trivalent Lanthanide in LaF_3 ," Argonne National Laboratory Report, (1977).
13. Dieter Kuze, Z. Physik 203, 49 (1967).
14. M.M. Abraham, L.A. Boatner, and M. Rappaz (in preparation).
15. M. Dzionara, H.G. Kahle, and F. Schedewie, Phys. Stat. Sol. (b) 47, 135 (1971).

Table I

Er ³⁺ :LuPO ₄											Er ³⁺ :HfSiO ₄										
Sym	Energy (cm ⁻¹)		Splitting Factors				Eigenvector Composition				Sym	Energy (cm ⁻¹)		Splitting Factors				Eigenvector Composition			
			g		g _⊥		SLQ(2J, 2J _z)		SLQ(2J, 2J _z)					g		g _⊥		SLQ(2J, 2J _z)		SLQ(2J, 2J _z)	
	cal	obs	cal	obs	cal	obs	%	largest	%	second		cal	obs	cal	obs	cal	obs	%	largest	%	second
Γ ₇	-1	0	6.77	6.39 ^a	4.94	4.97 ^a	71	4I (15, 7)	9	4I (15, -1)	Γ ₇	-1	0	3.77	4.32 ^b	6.81	6.68 ^b	41	4I (15, 7)	25	4I (15, -9)
Γ ₆	35	36	3.31		7.92		68	4I (15, 5)	22	4I (15, -3)	Γ ₇	28		7.14		.28		59	4I (15, 15)	34	4I (15, -9)
Γ ₇	49	53	-7.14		3.97		78	4I (15, -9)	8	4I (15, 7)	Γ ₆	39	30	-3.34		7.93		44	4I (15, 5)	27	4I (15, -3)
Γ ₇	100	98	16.05		.75		83	4I (15, 15)	10	4I (15, 7)	Γ ₇	58	59	4.31		6.30		45	4I (15, 7)	30	4I (15, -9)
Γ ₆	132		-5.79		5.87		45	4I (15, -11)	29	4I (15, -3)	Γ ₆	100		-5.97		3.49		65	4I (15, -11)	22	4I (15, 5)
Γ ₆	229		-7.17		.53		47	4I (15, -11)	42	4I (15, -3)	Γ ₆	165		12.31		3.68		80	4I (15, 13)	6	4I (15, -3)
Γ ₇	246		-1.33		9.33		82	4I (15, -1)	8	4I (15, -9)	Γ ₆	271		-1.25		8.11		63	4I (15, -3)	24	4I (15, 5)
Γ ₆	286		14.39		1.51		88	4I (15, 13)	6	4I (15, 5)	Γ ₇	298		-.87		9.33		81	4I (15, -1)	9	4I (15, 7)
Γ ₆	6548	6535	2.69		6.90		60	4I (13, 5)	32	4I (13, -3)	Γ ₆	6541	6548	9.10		3.75		58	4I (13, 13)	25	4I (13, 5)
Γ ₇	6556	6544	4.04		4.96		65	4I (13, 7)	25	4I (13, -1)	Γ ₇	6542	6530	.20		6.55		47	4I (13, 7)	32	4I (13, -9)
Γ ₇	6608	6602	-5.32		4.39		68	4I (13, -9)	22	4I (13, 7)	Γ ₆	6564	6564	3.02		.74		36	4I (13, 13)	21	4I (13, -3)
Γ ₆	6619	6615	8.63		2.83		68	4I (13, 13)	21	4I (13, -3)	Γ ₇	6576	6580	-2.86		6.23		59	4I (13, -9)	39	4I (13, 7)
Γ ₆	6647	6641	2.23		1.97		30	4I (13, 5)	26	4I (13, 13)	Γ ₆	6600	6597	-6.59		2.18		68	4I (13, -11)	25	4I (13, 5)
Γ ₇	6687	6682	-2.00		7.14		65	4I (13, -1)	21	4I (13, -9)	Γ ₆	6712		-1.02		6.64		64	4I (13, -3)	29	4I (13, 5)
Γ ₆	6697	6695	-9.00		2.08		70	4I (13, -11)	23	4I (13, -3)	Γ ₇	6728		-.64		7.40		79	4I (13, -1)	12	4I (13, 7)
Γ ₆	10198	10206	1.29		5.45		46	4I (11, 5)	34	4I (11, -3)	Γ ₆	10183		-9.75		.58		73	4I (11, -11)	13	2H2(11, -11)
Γ ₇	10211	10221	3.57		3.45		50	4I (11, 7)	28	4I (11, -1)	Γ ₇	10194	10189	.83		4.51		44	4I (11, 7)	25	4I (11, -9)
Γ ₆	10240	10244	-5.81		2.19		49	4I (11, -11)	20	4I (11, 5)	Γ ₆	10206	10209	1.36		4.64		52	4I (11, 5)	21	4I (11, -3)
Γ ₇	10246	10252	-1.47		1.36		31	4I (11, -9)	26	4I (11, 7)	Γ ₇	10209		-3.16		4.23		52	4I (11, -9)	29	4I (11, 7)
Γ ₆	10257	10256	-4.38		3.25		34	4I (11, -3)	30	4I (11, -11)	Γ ₆	10279		-.50		5.18		54	4I (11, -3)	26	4I (11, 5)
Γ ₇	10272	10274	-4.94		3.81		46	4I (11, -9)	29	4I (11, -1)	Γ ₇	10290		-.55		5.61		69	4I (11, -1)	12	2H2(11, -1)
Γ ₆	12363	12372	2.65	3.10	3.55	3.07	39	4I (9, 5)	13	4I (9, -3)	Γ ₆	12332	12327	2.20		3.83		35	4I (9, 5)	16	4I (9, -3)
Γ ₇	12429	12442	-6.97	-8.25	1.10	3.33	44	4I (9, -9)	14	2H2(9, -9)	Γ ₇	12413		-6.97		1.21		47	4I (9, -9)	15	2H2(9, -9)
Γ ₆	12432	12432	-.92	-1.64	3.55	3.17	39	4I (9, -3)	13	4I (9, 5)	Γ ₆	12443		-.46		3.83		34	4I (9, -3)	16	4I (9, 5)
Γ ₇	12508	12531	1.47		.78		23	4I (9, 7)	23	4I (9, -1)	Γ ₇	12451	12448	3.18		.16		34	4I (9, 7)	12	4I (9, -1)
Γ ₇	12578	12586	2.74		2.60		27	4I (9, 7)	22	4I (9, -1)	Γ ₇	12536		1.11		3.48		32	4I (9, -1)	16	4I (9, 7)

Table I Continued

Er ³⁺ :LuPO ₄										Er ³⁺ :HfSiO ₄											
Sym	Energy (cm ⁻¹)		Splitting Factors				Eigenvector Composition				Sym	Energy (cm ⁻¹)		Splitting Factors				Eigenvector Composition			
	cal	obs	g	g _⊥	obs	%	largest	%	second	cal		obs	g	g _⊥	obs	%	largest	%	second		
Γ ₇	15261	15235	4.11		3.05	3.02	37 4F (9, 7)	18 4F (9, -1)		Γ ₇	15213	15200	1.76		4.19	4.10	37 4F (9, -1)	20 4F (9, 7)			
Γ ₆	15290	15271	1.25	1.95	5.25		30 4F (9, 5)	28 4F (9, -3)		Γ ₆	15220	15235	.86	1.44	5.21	4.99	31 4F (9, -3)	27 4F (9, 5)			
Γ ₇	15301	15277	-7.44		2.21		48 4F (9, -9)	22 4I (9, -9)		Γ ₇	15297	15310	4.59	3.82	.82	.40	38 4F (9, 7)	17 4F (9, -1)			
Γ ₇	15336	15320	-.15	.40	4.84		38 4F (9, -1)	17 4I (9, -1)		Γ ₆	15319	15291	1.41		5.18		30 4F (9, 5)	26 4F (9, -3)			
Γ ₆	15378	15363	1.00		5.22		30 4F (9, -3)	28 4F (9, 5)		Γ ₇	15369	15357	-9.84		.63		56 4F (9, -9)	24 4I (9, -9)			
Γ ₆	18367	18364	-5.25	-5.33	.00	.16	66 4S (3, -3)	18 2P (3, -3)		Γ ₇	18335	18340	-1.74	-1.00	3.41		66 4S (3, -1)	18 2P (3, -1)			
Γ ₇	18396	18404	-1.73	-1.97	3.42	3.35	67 4S (3, -1)	18 2P (3, -1)		Γ ₆	18383	18381	-5.38	-4.50	.01		66 4S (3, -3)	18 2P (3, -3)			
Γ ₆	19102	19078	2.34	3.07	6.18	6.01	28 2H2(11, 5)	23 4G (11, 5)		Γ ₆	19114		1.26		6.33		23 2H2(11, 5)	20 2H2(11, -3)			
Γ ₇	19135		5.05		2.86		31 2H2(11, 7)	25 4G (11, 7)		Γ ₇	19134	19135	2.72		4.69		22 2H2(11, -1)	20 2H2(11, 7)			
Γ ₆	19165	19140	-11.05	-10.00	.61	.48	40 2H2(11,-11)	32 4G (11,-11)		Γ ₆	19155	19146	-11.33	-8.00	.19	.20	42 2H2(11,-11)	33 4G (11,-11)			
Γ ₇	19190	19178	-3.15	6.30	.77	.34	20 2H2(11, -9)	15 2H2(11, -1)		Γ ₇	19188	19189	-2.00		3.10		21 2H2(11, -9)	17 2H2(11, 7)			
Γ ₆	19193	19198	-1.37	.08	5.55	5.80	27 2H2(11, -3)	21 4G (11, -3)		Γ ₆	19204		.06		6.12		25 2H2(11, -3)	19 2H2(11, 5)			
Γ ₇	19223		-5.26		4.73		25 2H2(11, -9)	19 4G (11, -9)		Γ ₇	19224	19217	-4.08		5.21		23 2H2(11, -9)	17 4G (11, -9)			
Γ ₆	20493	20483	-2.74	-2.90	2.47	2.04	83 4F (7, -3)	8 4F (7, 5)		Γ ₆	20438	20424	-3.11	-3.23	2.00	1.23	86 4F (7, -3)	5 4F (7, 5)			
Γ ₇	20504		8.42		.03		91 4F (7, 7)	4 2G1(7, 7)		Γ ₇	20467	20493	-.95		4.72		89 4F (7, -1)	4 2G1(7, -1)			
Γ ₆	20560	20554	5.10		2.52		83 4F (7, 5)	8 4F (7, -3)		Γ ₆	20534	20535	5.55		2.08		86 4F (7, 5)	5 4F (7, -3)			
Γ ₇	20565	20561	-1.04		4.76		91 4F (7, -1)	4 2G1(7, -1)		Γ ₇	20561	20564	8.27		.10		89 4F (7, 7)	4 2G1(7, 7)			
Γ ₆	22149	22154	3.49		1.49		67 4F (5, 5)	15 4F (5, -3)		Γ ₆	22142	22126	-.59		1.80	1.62	51 4F (5, -3)	29 4F (5, 5)			
Γ ₇	22176	22182	-1.08		3.06		83 4F (5, -1)	12 2D1(5, -1)		Γ ₇	22150	22155	-1.16	-1.70	3.15		84 4F (5, -1)	12 2D1(5, -1)			
Γ ₆	22177	22192	-1.41		1.94		68 4F (5, -3)	14 4F (5, 5)		Γ ₆	22199	22215	2.13		2.42		52 4F (5, 5)	31 4F (5, -3)			
Γ ₆	22522		-2.18		.40		60 4F (3, -3)	20 2D1(3, -3)		Γ ₇	22458		-.70		1.53		61 4F (3, -1)	20 2D1(3, -1)			
Γ ₇	22537	22541	-.82		1.45		62 4F (3, -1)	20 2D1(3, -1)		Γ ₆	22564		-1.68		.54		59 4F (3, -3)	20 2D1(3, -3)			
Γ ₆	24487	24492	3.26	5.01	4.22	2.01	18 4F (9, 5)	14 2G1(9, 5)		Γ ₆	24418	24423	2.24	2.70	4.72	4.50	15 4F (9, 5)	12 2G1(9, 5)			
Γ ₇	24540	24539	-8.53		1.19		21 4F (9, -9)	16 2G1(9, -9)		Γ ₆	24507		-.10		4.73		15 4F (9, -3)	11 2G1(9, -3)			
Γ ₆	24547	24530	-1.15		4.21		18 4F (9, -3)	14 2G1(9, -3)		Γ ₇	24513	24512	.04	.80	4.27		12 4F (9, -1)	9 2G1(9, -1)			
Γ ₇	24601	24620	2.44		.84		11 4F (9, 7)	9 2G1(9, 7)		Γ ₇	24541	24552	-5.86		2.42		18 4F (9, -9)	14 2G1(9, -9)			

Table I Continued

Er ³⁺ :LuPO ₄										Er ³⁺ :HfSiO ₄											
Sym	Energy		Splitting Factors				Eigenvector Composition				Sym	Energy		Splitting Factors				Eigenvector Composition			
	(cm ⁻¹)		g		g _⊥		SLQ(2J,2J _z)		(cm ⁻¹)			g		g _⊥		SLQ(2J,2J _z)					
	cal	obs	cal	obs	cal	obs	% largest	% second	cal	obs		cal	obs	cal	obs	% largest	% second				
Γ ₇	24665	24653	2.83		3.35		11 4F (9, 7)	11 4F (9, -1)	Γ ₇	24594	24615	2.58		3.51		11 4F (9, 7)	11 4F (9, -1)				
Γ ₆	26295	26294	.91	1.00	6.45	5.83	29 4G (11, 5)	25 4G (11, -3)	Γ ₆	26243	26226	-1.19	1.54	6.29		29 4G (11, -3)	24 4G (11, 5)				
Γ ₇	26318	26317	2.85		5.09	5.26	28 4G (11, 7)	25 4G (11, -1)	Γ ₇	26259	26248	.75	2.10	6.13		36 4G (11, -1)	17 2H2(11, -1)				
Γ ₆	26357	26343	-11.47	-10.58	.04		53 4G (11,-11)	24 2H2(11,-11)	Γ ₆	26317	26322	-10.82	-9.75	.13	.72	51 4G (11,-11)	24 2H2(11,-11)				
Γ ₇	26393	26396	-4.14	-6.30	4.07		36 4G (11, -9)	18 4G (11, 7)	Γ ₇	26370		-1.96		4.86		30 4G (11, -9)	25 4G (11, 7)				
Γ ₆	26440	26459	-.09		6.40		33 4G (11, -3)	23 4G (11, 5)	Γ ₆	26410	26389	.33		6.38		28 4G (11, -3)	27 4G (11, 5)				
Γ ₇	26459	26478	-2.13		6.12		29 4G (11, -1)	18 4G (11, -9)	Γ ₇	26436	26401	-2.23		5.86		22 4G (11, -9)	20 4G (11, -1)				
Γ ₇	27343	27346	4.22		2.67		48 4G (9, 7)	27 4G (9, -1)	Γ ₇	27317	27313	-2.74		4.13		31 4G (9, -9)	29 4G (9, -1)				
Γ ₆	27350	27357	1.64	4.14	5.20		43 4G (9, 5)	34 4G (9, -3)	Γ ₇	27322	27327	.28		3.27		43 4G (9, 7)	31 4G (9, -9)				
Γ ₇	27358		-5.67		1.65		53 4G (9, -9)	13 4G (9, 7)	Γ ₆	27334	27331	2.41		5.05		49 4G (9, 5)	28 4G (9, -3)				
Γ ₆	27383	27402	.68	3.33	5.00		43 4G (9, -3)	34 4G (9, 5)	Γ ₆	27357	27381	-.17		4.77		49 4G (9, -3)	27 4G (9, 5)				
Γ ₇	27386	27398	-2.01		4.34		40 4G (9, -1)	23 4G (9, -9)	Γ ₇	27369	27387	-1.02		4.61		48 4G (9, -1)	15 4G (9, 7)				
Γ ₇	27496		-.21		7.83		52 2K (15, -1)	23 2K (15, 7)	Γ ₆	27485		11.89		2.38		77 2K (15, 13)	5 2K (15, 5)				
Γ ₆	27498		-.09		7.78		45 2K (15, -3)	35 2K (15, 5)	Γ ₇	27509		14.24		.60		77 2K (15, 15)	4 2L (15, 15)				
Γ ₆	27641		3.44		5.81		44 2K (15, 13)	29 2K (15,-11)	Γ ₆	27528		-8.52		1.66		70 2K (15,-11)	10 2K (15, -3)				
Γ ₇	27663		-1.23		6.69		48 2K (15, -9)	35 2K (15, 7)	Γ ₇	27556		-3.06		6.26		47 2K (15, -9)	23 2K (15, -1)				
Γ ₆	27682		.70		5.64		41 2K (15,-11)	36 2K (15, 13)	Γ ₆	27670		.49		7.25		44 2K (15, 5)	27 2K (15, -3)				
Γ ₇	27725		12.50		.03		72 2K (15, 15)	7 2K (15, -9)	Γ ₇	27674		.83		6.19		50 2K (15, 7)	33 2K (15, -9)				
Γ ₆	27783		.06		7.61		37 2K (15, -3)	36 2K (15, 5)	Γ ₇	27891		-.09		5.76		30 2K (15, -1)	19 4G (7, -1)				
Γ ₇	27789		.86		7.27		34 2K (15, -1)	31 2K (15, 7)	Γ ₆	27891		.13		1.76		24 4G (7, -3)	15 2G1(7, -3)				
Γ ₆	27953		1.41		3.30		23 4G (7, 5)	17 4G (7, -3)	Γ ₆	27915		1.94		4.70		26 2K (15, -3)	18 4G (7, 5)				
Γ ₇	27972		1.09		2.78		30 4G (7, -1)	18 2G1(7, -1)	Γ ₇	27941		6.59		.30		37 4G (7, 7)	22 2G1(7, 7)				
Γ ₇	27981		5.49		1.01		29 4G (7, 7)	17 2G1(7, 7)	Γ ₇	27966		-.02		5.54		27 2K (15, -1)	18 4G (7, -1)				
Γ ₆	27986		.47		3.48		22 4G (7, -3)	17 4G (7, 5)	Γ ₆	27967	27984	.10		5.26		20 2K (15, -3)	14 4G (7, -3)				

^afrom reference 8, ^breference 5

Table II. Crystal Field Parameters (cm^{-1}) for Er^{3+} in:

Parameter	LuPO_4	YPO_4	HfSiO_4
F^2	97015	97058	97537
F^4	69141	69142	68528
F^6	48232	48232	49052
ζ	2366	2368	2367
B_0^2	146	279	-531
B_0^4	68	155	404
B_4^4	-760	-756	-927
B_0^6	-643	-537	-464
B_4^6	-89	-141	-4
F^0	44051	44062	44134
α^*	15.9	15.9	15.9
β^*	632.0	632.0	632.0
γ^*	2017.	2017.	2017.
T^{2*}	157.5	157.5	157.5
T^{3*}	48.0	48.0	48.0
T^{4*}	18.0	18.0	18.0
T^{6*}	-342.0	-342.0	-342.0
T^{7*}	214.0	214.0	214.0
T^{8*}	449.0	449.0	449.0
M^{0*}	4.5	4.5	4.5
M^{2*}	2.52	2.52	2.52
M^{4*}	1.71	1.71	1.71
P^{2*}	667.0	667.0	667.0
P^{6*}	500.3	500.3	500.3
σ	13.2	14.7	14.5

* from reference 12

